

NON-MONOTONIC OPTIMAL DAMPER PLACEMENT VIA STEEPEST DIRECTION SEARCH

IZURU TAKEWAKI^{1,*‡}, SHINTA YOSHITOMI^{1,†§}, KOJI UETANI^{1,¶} AND MASAOKI TSUJI^{2,||}

¹*Department of Architecture and Architectural Systems, Kyoto University, Sakyo, Kyoto 606-8501, Japan*

²*Department of Architecture and Design, Kyoto Institute of Technology, Sakyo, Kyoto 606, Japan*

SUMMARY

An efficient and systematic procedure is proposed for finding the optimal damper positioning to minimize the dynamic compliance of a 3-D shear building model. The dynamic compliance is expressed in terms of the transfer function amplitudes of the local interstorey drifts evaluated at the undamped fundamental natural frequency. The dynamic compliance is minimized subject to a constraint on the sum of the damping coefficients of added dampers. Optimality criteria are derived and the optimal damper positioning is determined via an original steepest direction search algorithm. This algorithm enables one to find an optimal damper positioning sequentially for gradually increasing damper capacity levels. A non-monotonic design path with respect to the total damper capacity level often appears in the application of this algorithm. A new augmented algorithm via parameter switching is devised to find this non-monotonic design path. Copyright © 1999 John Wiley & Sons, Ltd.

KEY WORDS: optimal damper placement; passive control; dynamic compliance; transfer function; non-proportional damping; design sensitivity analysis; non-monotonic path

1. INTRODUCTION

The problem treated in the present paper is to find the optimal damper positioning to minimize the dynamic compliance of a 3-D shear building model. The dynamic compliance is defined as the sum of the transfer function amplitudes of the local interstorey drifts evaluated at the undamped fundamental natural frequency of the shear building model. Such objective function is minimized subject to a constraint on the sum of the damper capacities. An efficient and systematic algorithm is proposed for the optimal damper positioning. The features of the present formulation are as

* Correspondence to: Izuru Takewaki, Department of Architecture and Architectural Systems, Kyoto University, Sakyo, Kyoto 606-8501, Japan. E-mail: takewaki@archi.kyoto-u.ac.jp

‡ Associate Professor

† Currently at Obayashi Corporation

§ Graduate Student

¶ Professor

|| Research Associate

Contract/grant sponsor: Ministry of Education, Science and Culture of Japan; Contract/grant numbers: 07650659, 10555201, 10650562

follows: to deal with any damping system, e.g. Voigt-type or Maxwell-type, proportional or non-proportional, to treat any structural system so far as it can be modelled with finite-element systems and to consist of a systematic algorithm without any indefinite iterative operation. While a different algorithm was devised and a variation from a *uniform* storeywise distribution of added dampers was considered in the former paper,¹ a variation from the null state is treated in the present paper. This path helps designers to understand simultaneously which position would be the best and what capacity of dampers would be required to attain a series of desired response performance levels. In the fundamental algorithm proposed here, sometimes negative damping coefficients are required to satisfy the optimality conditions. To avoid this unrealistic situation, a new augmented algorithm via *parameter switching* is presented.

While research on active and passive control is being conducted extensively,²⁻⁶ research on optimal passive damper placement is very limited. Comprehensive reviews for this problem are provided.³⁻⁶ The following studies may be relevant to the present paper. Constantinou and Tadjbakhsh⁷ derived the optimum damping coefficient for a damper placed on the first storey of a shear building subjected to horizontal random earthquake motions. Gurgoze and Muller⁸ presented a numerical method for finding the optimal placement and the optimal damping coefficient for a single viscous damper in a prescribed linear multi-degree-of-freedom system. Zhang and Soong⁹ proposed a seismic design method to find the optimal configuration of viscous dampers for a building with specified storey stiffnesses. While their method is based upon a heuristic criterion that an additional damper should be placed sequentially on the storey with the maximum interstorey drift, it is simple, realistic and pioneering. Hahn and Sathiyaveeswaran¹⁰ performed several parametric studies on the effects of damper distribution on the earthquake response of shear buildings, and showed that, for a building with uniform storey stiffnesses, dampers should be added to the lower half-floors of the building. De Silva¹¹ presented a gradient algorithm for the optimal design of discrete passive dampers in the vibration control of a class of flexible systems. Inaudi and Kelly¹² proposed a procedure for finding the optimal isolation damping for minimum acceleration response of base-isolated structures subjected to stationary random excitation. Tsuji and Nakamura¹³ proposed an algorithm to find both the optimal storey stiffness distribution and the optimal damper distribution for a shear building model subjected to a set of spectrum-compatible earthquakes. Moreover, Tsuji and Nakamura¹⁴ proposed a method for taking into account the support-member flexibility in the stiffness design of a shear building model with added viscous dampers. Masri *et al.*¹⁵ presented a simple yet efficient optimum active control method for reducing the oscillations of distributed parameter systems subjected to arbitrary deterministic or stochastic excitations. While they deal with active control, the result is informative to the development in passive optimal control theories.

2. PROBLEM OF OPTIMAL DAMPER POSITIONING FOR 3-D SHEAR BUILDING MODELS

2.1. Modelling of a structure

Consider a three-dimensional (3-D) n -storey shear building model as shown in Figure 1. For simplicity of presentation, this model is assumed to have mono-eccentricity, and the lateral-torsional vibration only in the x -direction is considered. This model consists of m planar frames. It is assumed that added viscous dampers can be installed in all the storeys in every frame. The

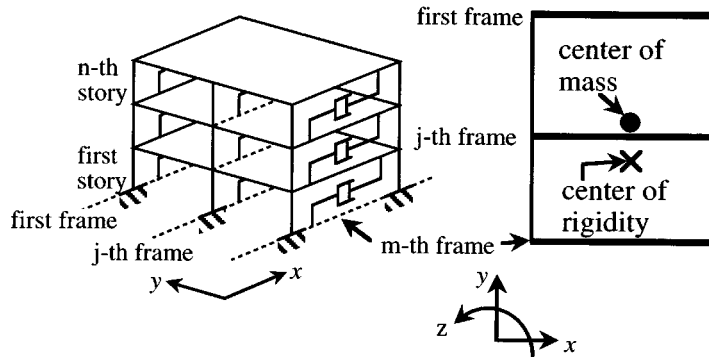


Figure 1. Three-dimensional (3-D) n -storey shear building model consisting of m planar frames

numbering of added dampers is made sequentially. Let c_i denote the damping coefficient of the i th added damper. The total number of added dampers is denoted by $N = n \times m$. An excitation in the x -direction is considered. The translational displacement of the centre of mass G in the x -direction and the angle of rotation of the floor around a vertical axis through G are the displacements to be considered. Let $\mathbf{u}(t)$ denote the generalized displacements in the system co-ordinate system and let \mathbf{M} denote the system mass matrix of the model. All the member stiffnesses of the model are given and its system stiffness matrix is described by \mathbf{K} . The structural damping of the model is considered and the system damping matrix due to this structural damping is given by \mathbf{C} . The undamped fundamental natural circular frequency of the model in the x -direction is denoted by ω_1 .

2.2. Problem of optimal damper positioning

When this 3-D shear building model without added dampers is subjected to a horizontal base acceleration $\ddot{u}_g(t)$ in the x -direction, the equation of motion for this model can be written as

$$\mathbf{K}\mathbf{u}(t) + \mathbf{C}\dot{\mathbf{u}}(t) + \mathbf{M}\ddot{\mathbf{u}}(t) = -\mathbf{M}\mathbf{r}\ddot{u}_g(t) \quad (1)$$

where \mathbf{r} is the influence coefficient vector. See Reference 16, for example, for details of \mathbf{K} , \mathbf{C} , \mathbf{M} and \mathbf{r} .

Let $\mathbf{U}(\omega)$ and $\ddot{U}_g(\omega)$ denote the Fourier transforms of $\mathbf{u}(t)$ and $\ddot{u}_g(t)$, respectively. Fourier transformation of equation (1) may be reduced to the following form:

$$(\mathbf{K} + i\omega\mathbf{C} - \omega^2\mathbf{M})\mathbf{U}(\omega) = -\mathbf{M}\mathbf{r}\ddot{U}_g(\omega) \quad (2)$$

where i is the imaginary unit.

When the added dampers are included, equation (2) may be modified to the following form:

$$\{\mathbf{K} + i\omega(\mathbf{C} + \mathbf{C}_v) - \omega^2\mathbf{M}\}\mathbf{U}_v(\omega) = -\mathbf{M}\mathbf{r}\ddot{U}_g(\omega) \quad (3)$$

where \mathbf{C}_v is the damping matrix due to the added viscous dampers. In this paper it is assumed that the masses of dampers are negligible in comparison with floor masses. It is interesting to note that, since the present formulation is developed in the frequency range, it is possible to deal with various other damping systems in terms of complex stiffnesses.

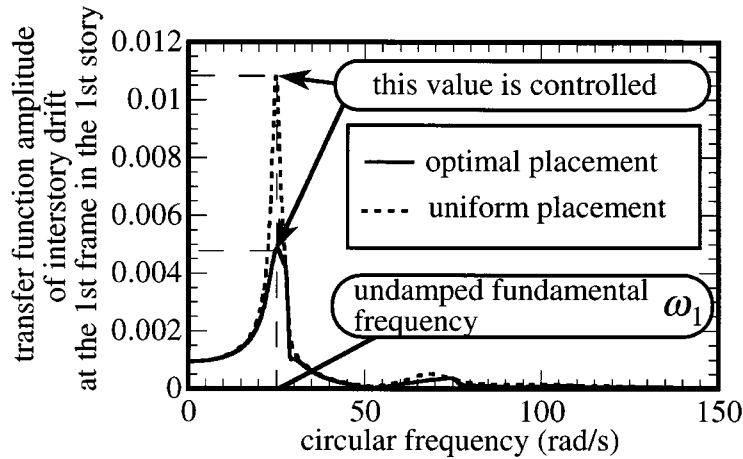


Figure 2. Transfer function amplitude of an interstorey drift with respect to excitation frequency and its value as evaluated at the undamped fundamental natural frequency

Let us define new quantities $\hat{\mathbf{U}}$ by

$$\hat{\mathbf{U}} \equiv \mathbf{U}_v(\omega_1)/\dot{\mathbf{U}}_g(\omega_1) \quad (4)$$

\hat{U}_i is equal to the value such that ω_1 is substituted in the frequency response function which can be obtained as $U_{vi}(\omega)$ after substituting $\dot{\mathbf{U}}_g(\omega) = 1$ in equation (3) (see Figure 2). This quantity has been utilized first in Reference 17 for structural redesign problems. While a steady-state resonant response at the fundamental natural frequency is treated here to explain the fundamental feature of the present optimization algorithm, optimization for random earthquake inputs with wide-band frequency contents will be shown elsewhere based on the present theory.¹⁸ It should be noted that, because \mathbf{M} and \mathbf{K} are prescribed, ω_1 is a given value. Due to equations (3) ($\omega = \omega_1$) and (4), $\hat{\mathbf{U}}$ must satisfy

$$\mathbf{A}\hat{\mathbf{U}} = -\mathbf{M}\mathbf{r} \quad (5)$$

where

$$\mathbf{A} = \mathbf{K} + i\omega_1(\mathbf{C} + \mathbf{C}_v) - \omega_1^2\mathbf{M} \quad (6)$$

Let $\hat{\delta}_i$ denote the transfer function at $\omega = \omega_1$ of the local interstorey drift at the location where the i th damper exists. $\hat{\boldsymbol{\delta}} = \{\hat{\delta}_i\}$ can be derived from $\hat{\mathbf{U}}$ by the transformation $\hat{\boldsymbol{\delta}} = \mathbf{T}\hat{\mathbf{U}}$ where \mathbf{T} is a constant matrix including given geometrical parameters only. The local interstorey drift will be simply called the interstorey drift hereafter.

It should be remarked here that the squares of the transfer function amplitudes are meaningful from physical points of view because they can be transformed into response mean squares (statistical quantities) after multiplication with the power spectral density function of a disturbance and integration in the frequency range. Since the transfer function amplitude of a nodal displacement evaluated at the undamped fundamental natural circular frequency can be related to the level of this response mean square, these transfer function amplitudes are treated as controlled quantities in the present paper.

The problem of optimal damper positioning for a 3-D shear building model may be described as follows:

Problem PODPT: Find the damping coefficients $\mathbf{c} = \{c_i\}$ of added dampers which minimize the sum of the transfer function amplitudes of the interstorey drifts evaluated at the undamped fundamental natural circular frequency ω_1

$$f(\mathbf{c}) = \sum_{i=1}^N |\hat{\delta}_i(\mathbf{c})| \quad (7)$$

subject to a constraint on the sum of the damping coefficients of added dampers

$$\sum_{i=1}^N c_i = \bar{W} \quad (\bar{W}: \text{specified value}) \quad (8a)$$

and to constraints on the damping coefficients of added dampers

$$0 \leq c_i \leq \bar{c}_i \quad (i = 1, \dots, N) \quad (8b)$$

where \bar{c}_i is the upper bound of the damping coefficient of the i th added damper.

The generalized Lagrangian L for Problem PODPT may be expressed in terms of Lagrange multipliers λ , $\boldsymbol{\mu} = \{\mu_i\}$, $\mathbf{v} = \{v_i\}$.

$$L(\mathbf{c}, \lambda, \boldsymbol{\mu}, \mathbf{v}) = f(\mathbf{c}) + \lambda \left(\sum_{i=1}^N c_i - \bar{W} \right) + \sum_{i=1}^N \mu_i (0 - c_i) + \sum_{i=1}^N v_i (c_i - \bar{c}_i) \quad (9)$$

For simplicity of expression argument (\mathbf{c}) will be omitted hereafter.

2.3. Optimality criteria

The principal optimality criteria for Problem PODPT without active upper and lower bound constraints on damping coefficients may be derived from stationarity conditions of the generalized Lagrangian L ($\boldsymbol{\mu} = \mathbf{0}$, $\mathbf{v} = \mathbf{0}$) with respect to \mathbf{c} and λ .

$$f_{,j} + \lambda = 0 \quad \text{for } 0 < c_j < \bar{c}_j \quad (j = 1, \dots, N) \quad (10)$$

$$\sum_{i=1}^N c_i - \bar{W} = 0 \quad (11)$$

Here and in the following $(\)_{,j}$ denotes the partial differentiation with respect to c_j . If constraints (8b) are active, equation (10) must be modified into the following forms:

$$f_{,j} + \lambda \geq 0 \quad \text{for } c_j = 0 \quad (12a)$$

$$f_{,j} + \lambda \leq 0 \quad \text{for } c_j = \bar{c}_j \quad (12b)$$

2.4. Solution algorithm

In the proposed procedure the model without added dampers, i.e. $c_j = 0$ ($j = 1, \dots, N$), is employed as the initial model. The damping coefficients of added dampers are *increased gradually*

via a new steepest direction search algorithm. Let Δc_i and $\Delta \bar{W}$ denote the increment of the damping coefficient of the i th added damper and the increment of the sum of the damping coefficients of added dampers, respectively. Given $\Delta \bar{W}$, the problem is to determine the effective position and amount of the increments of the damping coefficients of added dampers. To develop this algorithm, the first- and second-order sensitivities of the objective function with respect to a design variable are derived in the following.

Differentiation of equation (5) with respect to a design variable c_j provides

$$\mathbf{A}_{,j}\hat{\mathbf{U}} + \mathbf{A}\hat{\mathbf{U}}_{,j} = \mathbf{0} \quad (13)$$

From equation (6), $\mathbf{A}_{,j}$ may be expressed as follows:

$$\mathbf{A}_{,j} = i\omega_1 \mathbf{C}_{v,j} \quad (14)$$

Since \mathbf{A} is regular, the first-order sensitivities of $\hat{\mathbf{U}}$ are derived from equation (13) as

$$\hat{\mathbf{U}}_{,j} = -\mathbf{A}^{-1}\mathbf{A}_{,j}\hat{\mathbf{U}} \quad (15a)$$

The first-order sensitivities of the interstorey drift $\hat{\delta}$ are then expressed as

$$\hat{\delta}_{,j} = \mathbf{T}\hat{\mathbf{U}}_{,j} = -\mathbf{T}\mathbf{A}^{-1}\mathbf{A}_{,j}\hat{\mathbf{U}} \quad (15b)$$

The quantity $\hat{\delta}_i$ may be rewritten formally as

$$\hat{\delta}_i = \text{Re}[\hat{\delta}_i] + i \text{Im}[\hat{\delta}_i] \quad (16)$$

where $\text{Re}[\]$ and $\text{Im}[\]$ indicate the real and imaginary parts, respectively, of a complex number. The first-order sensitivity of $\hat{\delta}_i$ may be formally expressed as

$$\hat{\delta}_{i,j} = (\text{Re}[\hat{\delta}_i])_{,j} + i(\text{Im}[\hat{\delta}_i])_{,j} \quad (17)$$

The absolute value of $\hat{\delta}_i$ is defined by

$$|\hat{\delta}_i| = \sqrt{(\text{Re}[\hat{\delta}_i])^2 + (\text{Im}[\hat{\delta}_i])^2} \quad (18)$$

The first-order sensitivity of $|\hat{\delta}_i|$ may then be expressed as

$$|\hat{\delta}_{i,j}| = \frac{1}{|\hat{\delta}_i|} \{ \text{Re}[\hat{\delta}_i](\text{Re}[\hat{\delta}_i])_{,j} + \text{Im}[\hat{\delta}_i](\text{Im}[\hat{\delta}_i])_{,j} \} \quad (19)$$

where $(\text{Re}[\hat{\delta}_i])_{,j}$ and $(\text{Im}[\hat{\delta}_i])_{,j}$ are calculated from equations (15b) and (17).

A general expression $|\hat{\delta}_{i,jl}|$ is derived here for the purpose of developing a solution procedure for Problem PODPT. Differentiation of equation (19) with respect to c_l leads to

$$\begin{aligned} |\hat{\delta}_{i,jl}| = \frac{1}{|\hat{\delta}_i|^2} \{ & |\hat{\delta}_i| \{ (\text{Re}[\hat{\delta}_i])_{,l}(\text{Re}[\hat{\delta}_i])_{,j} + \text{Re}[\hat{\delta}_i](\text{Re}[\hat{\delta}_i])_{,jl} + (\text{Im}[\hat{\delta}_i])_{,l}(\text{Im}[\hat{\delta}_i])_{,j} \\ & + \text{Im}[\hat{\delta}_i](\text{Im}[\hat{\delta}_i])_{,jl} \} - |\hat{\delta}_i|_{,l} \{ \text{Re}[\hat{\delta}_i](\text{Re}[\hat{\delta}_i])_{,j} + \text{Im}[\hat{\delta}_i](\text{Im}[\hat{\delta}_i])_{,j} \} \} \end{aligned} \quad (20)$$

$(\text{Re}[\hat{\delta}_i])_{,jl}$ and $(\text{Im}[\hat{\delta}_i])_{,jl}$ in equation (20) are found from

$$\hat{\delta}_{,jl} = \mathbf{T}\mathbf{A}^{-1}(\mathbf{A}_{,l}\mathbf{A}^{-1}\mathbf{A}_{,j}\hat{\mathbf{U}} - \mathbf{A}_{,j}\hat{\mathbf{U}}_{,l}) \quad (21)$$

which is derived by differentiating equation (15b) with respect to c_l and using the relation $\mathbf{A}_{,l}^{-1} = -\mathbf{A}^{-1}\mathbf{A}_{,l}\mathbf{A}^{-1}$. Substitution of equation (15a) into (21) leads to the following form:

$$\hat{\delta}_{,jl} = \mathbf{T}\mathbf{A}^{-1}(\mathbf{A}_{,l}\mathbf{A}^{-1}\mathbf{A}_{,j} + \mathbf{A}_{,j}\mathbf{A}^{-1}\mathbf{A}_{,l})\hat{\mathbf{U}} \quad (22)$$

The derivatives $|\hat{\delta}_i|_{,jl}$ are derived from equation (20). $(\text{Re}[\hat{\delta}_i])_{,j}$ and $(\text{Im}[\hat{\delta}_i])_{,j}$ in equation (20) are calculated from equation (15b) and $(\text{Re}[\hat{\delta}_i])_{,jl}$ and $(\text{Im}[\hat{\delta}_i])_{,jl}$ in equation (20) are found from equation (22).

The fundamental solution algorithm in the case of $c_j < \bar{c}_j$ for all j may be summarized as follows:

Step 0: Initialize all the added dampers as $c_j = 0$ ($j = 1, \dots, N$). In the initial state the damping considered is the structural damping alone in the model. Assume $\Delta\bar{W}$.

Step 1: Compute $f_{,i}$ by equation (19).

Step 2: Find the index k such that

$$-f_{,k} = \max_i \{-f_{,i}\} \quad (23)$$

Step 3: Update f by $f + f_{,k}\Delta c_k$ where $\Delta c_k = \Delta\bar{W}$.

Step 4: Update $f_{,i}$ by $f_{,i} + f_{,ik}\Delta c_k$ using equation (20).

Step 5: If in Step 4 there exists a damper of an index j such that the following condition is satisfied

$$-f_{,k} = \max_{j, j \neq k} \{-f_{,j}\} \quad (24)$$

then stop tentatively. Compute the corresponding $\Delta\tilde{c}_k$ and update $f_{,i}$ by $f_{,i} + f_{,ik}\Delta\tilde{c}_k$ using equation (20).

Step 6: Repeat Steps 2–5 until the constraint (8a), i.e. $\sum_{i=1}^N c_i = \bar{W}$, is satisfied.

The schematic diagram for this fundamental solution algorithm is shown in Figure 3. The relation between the first derivatives of the objective function and the damping coefficients is explained there in detail. Once the first derivative of the objective function starts to attain the maximum absolute value, the corresponding damper begins possessing a non-zero value. The dampers begin possessing non-zero damping coefficients in the order of c_1, c_4, c_2, c_3 in Figure 3.

In Steps 2 and 3 in the aforementioned algorithm, the direction which reduces the objective function most effectively under the condition $\sum_{i=1}^N \Delta c_i = \Delta\bar{W}$ is found and the design is updated in that direction. It is therefore appropriate to call the present algorithm 'the steepest direction search algorithm'. This algorithm may be similar to the well-known steepest descent method in the mathematical programming. However, while the conventional steepest descent method uses the gradient vector itself of the objective function as the direction and does not utilize optimality criteria, the present algorithm takes full advantage of the newly derived optimality criteria (10), (12a), (12b) and does not adopt the gradient vector as the direction. In other words, the steepest

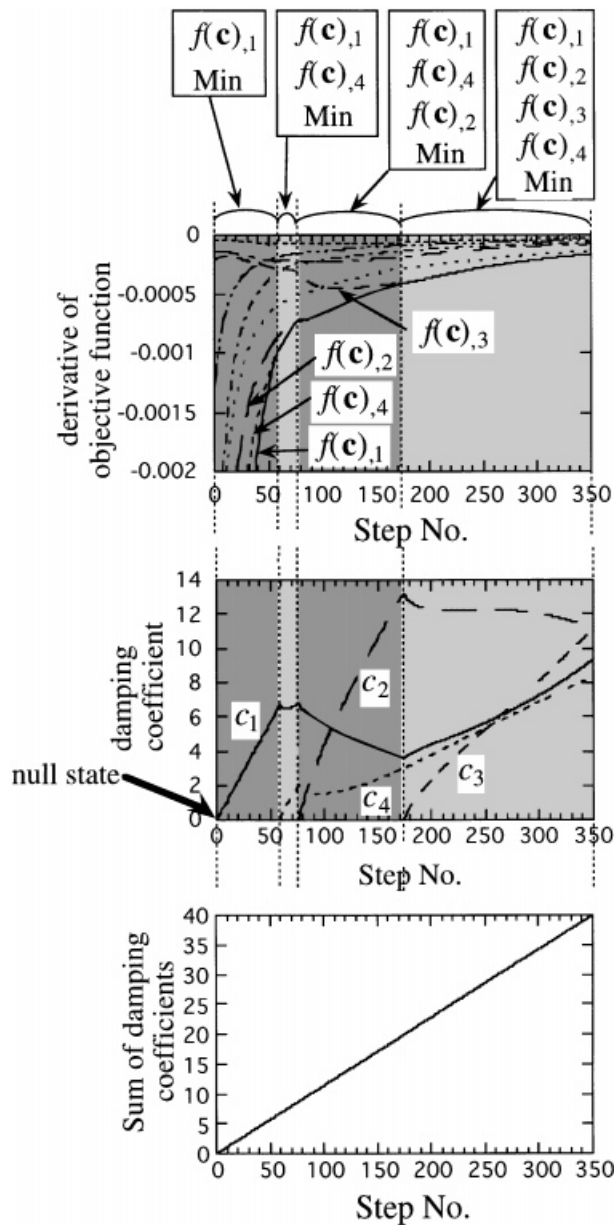


Figure 3. Schematic diagram of fundamental algorithm for optimal damper placement

direction search guarantees the automatic satisfaction of the optimality criteria. For example, if Δc_k is added to the k th added damper in which equation (23) is satisfied, then its damper ($c_k > 0$) satisfies the optimality condition (10) and the other dampers ($c_j = 0$, $j \neq k$) satisfy the optimality condition (12a). It should be noted that a series of subproblems is introduced here

tentatively in which the damper level \bar{W} is increased gradually by $\Delta\bar{W}$ from zero through the specified value.

If there exist multiple indices k_1, \dots, k_p in Step 2, f and $f_{,j}$ have to be updated by

$$f \rightarrow f + \sum_{i=k_1}^{k_p} f_{,i} \Delta c_i \quad (25a)$$

$$f_{,j} \rightarrow f_{,j} + \sum_{l=k_1}^{k_p} f_{,jl} \Delta c_l \quad (25b)$$

Furthermore the index k in Step 5 has to be replaced by the indices k_1, \dots, k_p . The ratios among the magnitudes Δc_i must be determined so that the following relations are satisfied:

$$f_{,k_1} + \sum_{i=k_1}^{k_p} f_{,k_1 i} \Delta c_i = \dots = f_{,k_p} + \sum_{i=k_1}^{k_p} f_{,k_p i} \Delta c_i \quad (26)$$

Equation (26) requires that the optimality condition (10) continues to be satisfied in the dampers with the indices k_1, \dots, k_p .

In the case where the damping coefficients of some added dampers attain their upper bounds, such constraints must be incorporated in the aforementioned algorithm. In that case the increment Δc_k is added subsequently to the damper in which $-f_{,k}$ attains the maximum among all the dampers except those attaining the upper bound.

3. NON-MONOTONIC PATH WITH RESPECT TO DAMPER LEVEL

In most cases, the increase of member stiffnesses reduces the response of a structure under disturbances with a wide-band frequency content. On the other hand, increase of damping coefficient of added dampers does not necessarily lead to the reduction of the response because of complicated damping characteristics. Non-proportional damping may cause further complicated phenomena. It has been found through numerical experiments that the algorithm mentioned above can lead to the appearance of negative damping coefficients. In the real world, negative damping coefficients are difficult to be understood and this situation is excluded with the constraints (8b). In this section a new method is proposed for preventing from appearance of negative damping coefficients and finding a path continuously within such complex design regions.

Figure 4(a) shows a situation at which a damping coefficient of a specifically added damper c_2 starts to attain a negative value. At this stage, the proposed augmented algorithm recommends to change the signs of the damping coefficients of the dampers satisfying the optimality condition (10). In the following step, the design parameter is switched from the total damper capacity level (sum of the damping coefficients) to the damping coefficient of that damper c_2 . In this range, the sum of the damping coefficients begins decreasing and afterwards begins to increase. It is noted that, while the increment of the sum of the damping coefficients has been specified in the range without the emergence of negative damping coefficients, it is obtained for a specified increment of the damping coefficient of that damper c_2 . The validity of this treatment is shown in the sequel.

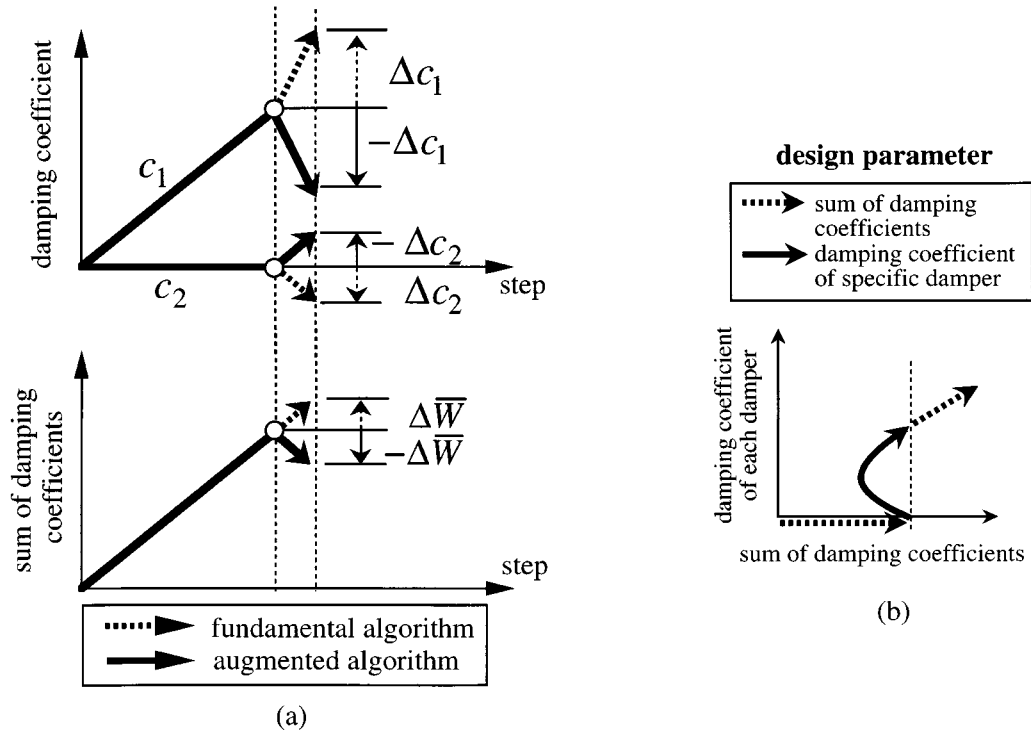


Figure 4. (a) Procedure for avoiding emergence of negative damping coefficients; (b) design parameters in non-monotonic design path

The optimality condition (10) is satisfied in the following form:

$$f(\mathbf{c})_{,k_1} = \dots = f(\mathbf{c})_{,k_p} \quad (27)$$

Let $\Delta \mathbf{c}$ denote the set of increments of the damping coefficients including a negative damping coefficient. In order for these optimality conditions to continue being satisfied for the increments $\Delta \mathbf{c}$, the following relations must be satisfied:

$$f(\mathbf{c} + \Delta \mathbf{c})_{,k_1} = \dots = f(\mathbf{c} + \Delta \mathbf{c})_{,k_p} \quad (28)$$

The first-order Taylor expansion of the first term may be written as

$$f(\mathbf{c} + \Delta \mathbf{c})_{,k_1} = f(\mathbf{c})_{,k_1} + \sum_{i=1}^p f(\mathbf{c})_{,k_1 k_i} \Delta \tilde{c}_{k_i} \quad (29)$$

From equation (29), the following conditions must be satisfied in order that equations (27) and (28) hold:

$$\sum_{i=1}^p f(\mathbf{c})_{,k_1 k_i} \Delta \tilde{c}_{k_i} = \dots = \sum_{i=1}^p f(\mathbf{c})_{,k_j k_i} \Delta \tilde{c}_{k_i} = \dots = \sum_{i=1}^p f(\mathbf{c})_{,k_p k_i} \Delta \tilde{c}_{k_i} \quad (30)$$

It should be noted that, if the damping coefficients of the dampers except a specific damper with a negative damping coefficient in the fundamental algorithm are relatively large, a new set $\mathbf{c} - \Delta\mathbf{c}$ does not include any negative damping coefficient. In order that the optimality conditions are satisfied for the newly designed variables $\mathbf{c} - \Delta\mathbf{c}$, the following relation must hold:

$$f(\mathbf{c} - \Delta\mathbf{c})_{,k_1} = \dots = f(\mathbf{c} - \Delta\mathbf{c})_{,k_p} \quad (31)$$

The first-order Taylor expansion of the first term may be written as

$$f(\mathbf{c} - \Delta\mathbf{c})_{,k_1} = f(\mathbf{c})_{,k_1} - \sum_{i=1}^p f(\mathbf{c})_{,k_1 k_i} \Delta \tilde{c}_{k_i} \quad (32)$$

From equations (27), (30) and (32), it is apparent that equations (31) hold. This guarantees the validity of the proposed new algorithm for avoiding negative damping coefficients.

After the sum of the damping coefficients returns to a value from which the damping coefficient of a specific damper starts to attain a negative value, the design parameter is re-switched from the damping coefficient of that damper to the sum of the damping coefficients (see Figure 4(b)).

4. NUMERICAL EXAMPLES

Consider a three-storey shear building model as shown in Figure 5. The shear building model consists of three planar frames with different storey stiffnesses. The centre of mass and center of rigidity in every floor coincide. Every floor mass and mass moment of inertia of the floor around a vertical axis are assumed to be $m = 294(\text{ton})$, $I = 1.96 \times 10^4 (\text{ton cm}^2)$. The element storey stiffnesses in the three frames are shown in Figure 5. The stiffness of the third frame is the strongest and the centre of rigidity is located slightly near to the third frame. The undamped fundamental natural circular frequency of the model is $\omega_1 = 24.8 (\text{rad/s})$. The structural damping of the shear building model is given by a critical damping ratio $= 0.02$ in the lowest eigenvibration. The numbering of the added dampers is shown in Figure 5. It is assumed that all the constraints on upper bounds of the damping coefficients are inactive, i.e. $c_j < \bar{c}_j$ for all j . The final level of the sum of the damping coefficients of the added dampers is $\bar{W} = 40 (\text{tonfs/cm})$. The increment of \bar{W} is given by $\Delta\bar{W} = \bar{W}/400$. In the non-monotonic range, 25 steps are required for the sum of the damping coefficients to return to the original value.

The distributions of the optimal damping coefficients obtained via the present fundamental procedure are plotted in Figure 6. It can be observed that the dampers are added in the order of c_1, c_4, c_2 and the damper c_3 begins to attain a negative damping coefficient around $\bar{W} = 27 (\text{tonfs/cm})$. This indicates that the optimal damper placement requires for added dampers to be placed in order to suppress the torsional vibration component. Figure 7 shows the distributions of the optimal damping coefficients obtained via the augmented procedure described in Section 3. The damping coefficient of damper c_3 is taken as a design parameter in the non-monotonic range. It is found that the modification by c_3 greatly influences the optimal damping distributions of dampers c_1, c_2 . It is also found that there exist multiple stationary solutions in the non-monotonic range. It is possible to obtain the optimal solution by comparing the objective functions of the

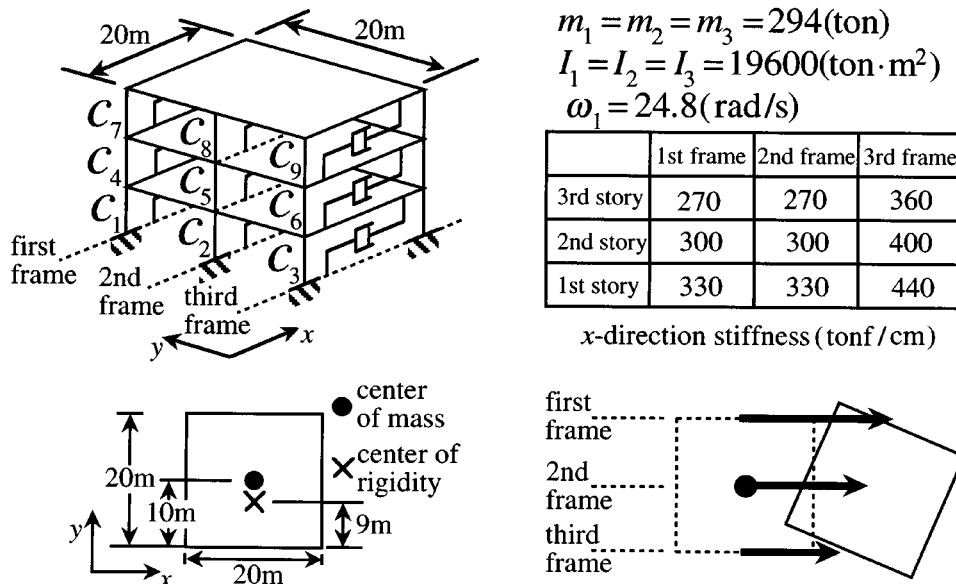


Figure 5. Three-storey shear building model consisting of three planar frames with added viscous dampers to be designed

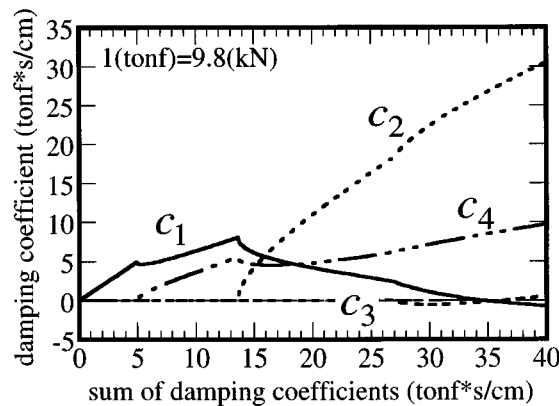


Figure 6. Variation of optimal damping coefficients with respect to the sum of damping coefficients (fundamental algorithm)

stationary solutions. Figure 8 shows the variation of the first-order derivatives of the objective function. Figure 9 illustrates the satisfaction level of the optimality conditions (10). The ordinate indicates the value of the left-hand side in equation (10) divided by λ . It can be observed from Figure 9 that the optimality criteria, equation (10) and inequality (12a), are satisfied in all the dampers for every \bar{W} .

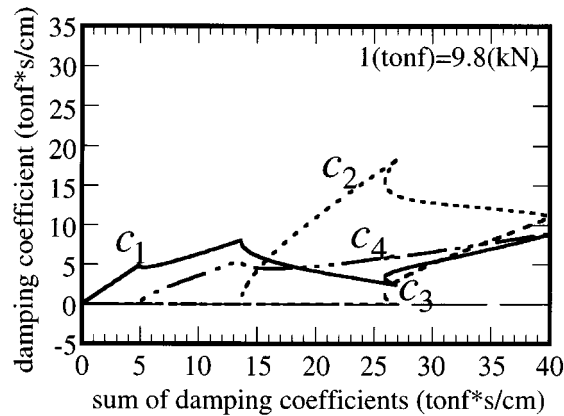


Figure 7. Variation of optimal damping coefficients with respect to the sum of damping coefficients (augmented algorithm)

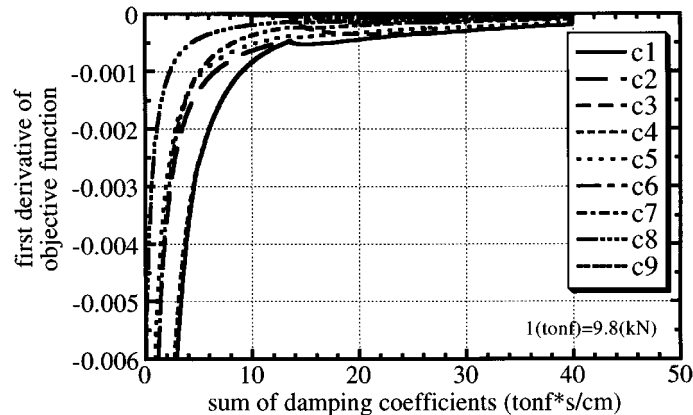


Figure 8. Variation of first-order design sensitivities of the objective function with respect to the sum of damping coefficients

Figure 10 shows the variations of the lowest-mode damping ratio for the optimal placement and the uniform placement. The uniform placement means the case where the same increment $\Delta\bar{W}/9$ of the damping coefficient is added to every damper. It can be seen that the optimal placement increases the lowest-mode damping ratio more effectively than the uniform placement. Figure 11 illustrates the objective function with respect to the sum of the damping coefficients for the optimal placement and the uniform placement. The optimal placement actually reduces the objective function more rapidly than the uniform placement especially in the lower damping capacity level. Figure 12 shows the sum of the seismic-response interstorey drifts corresponding to the objective function. Each transfer function amplitude of the local interstorey drift has been replaced by the mean peak local interstorey drift to the design earthquakes represented by the response spectrum due to Newmark and Hall.¹⁹ The response spectrum method by Yang *et al.*²⁰

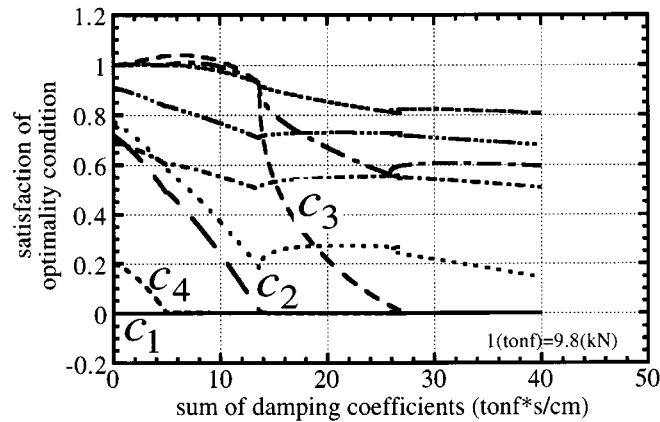


Figure 9. Satisfaction level of optimality conditions, equation (10) and inequality (12a)

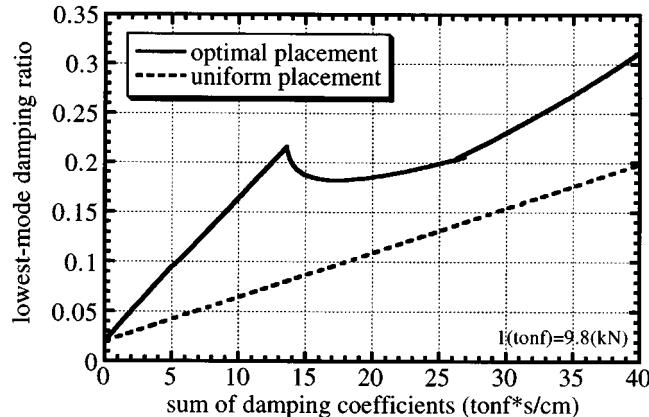


Figure 10. Variation of the lowest-mode damping ratio with respect to the sum of damping coefficients (optimal placement and uniform placement)

for a non-proportional damping has been employed to estimate the mean peak local interstorey drift. It can be found from Figure 12 that in a certain narrow range, the seismic response of the model designed optimally for the steady-state resonant response becomes larger than that for the uniform placement. Higher-mode effects on seismic responses to wide-band inputs and non-proportional damping effects may be a cause of this phenomenon. Direct introduction of the seismic response into the objective function (7) and the application of the random vibration theories in the seismic response evaluation may lead to a more realistic optimal damper placement.¹⁸ Numerical integration in the frequency range and sensitivity expressions of frequency response functions will be required in the computation. However, this treatment may require unrealistic computational resources.

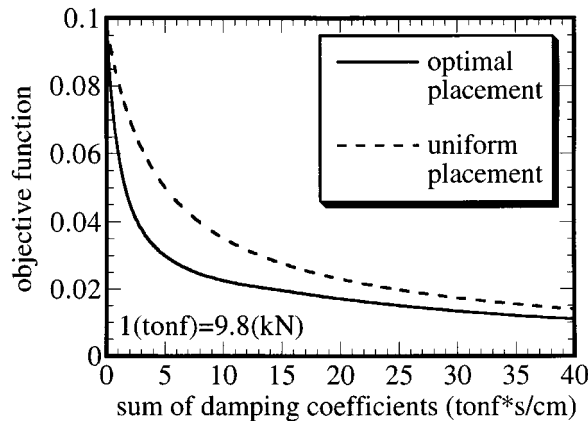


Figure 11. Variation of the objective function with respect to the sum of damping coefficients (optimal placement and uniform placement)

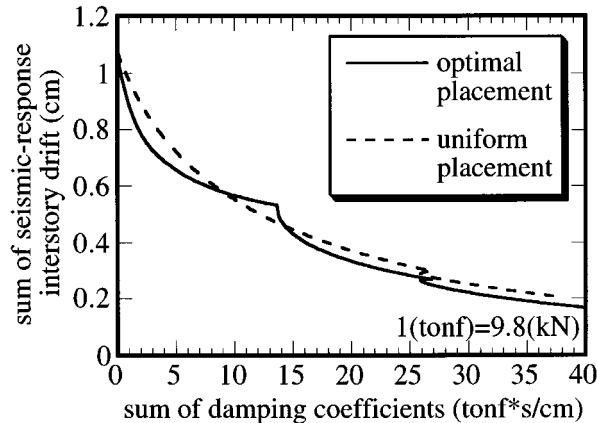


Figure 12. Variation of the sum of the seismic-response interstorey drifts with respect to the sum of damping coefficients (optimal placement and uniform placement)

5. CONCLUSIONS

An efficient and systematic procedure called a steepest direction search algorithm has been proposed for finding the optimal damper positioning in a 3-D shear building model. This problem is aimed at minimizing the sum of the transfer function amplitudes of the local interstorey drifts evaluated at the undamped fundamental natural frequency subject to a constraint on the sum of the damping coefficients of added dampers. The optimal damper positioning is determined based upon the optimality criteria. The features of the present formulation are as follows: to deal with any damping system, e.g. Voigt-type or Maxwell-type, proportional or nonproportional; to treat any structural system so far as it can be modelled with finite-element systems and to consist of a systematic algorithm without any indefinite iterative operation. A new

algorithm to avoid the emergence of negative damping coefficients has been devised. Efficiency and reliability of the present procedure have been demonstrated through an example.

The support-member stiffness may affect the optimal damper positioning and the response suppression level due to added viscous dampers. This stiffness should be taken into account in the design of magnitude and the positioning of the added dampers. The Maxwell-type damper-spring model, a proper model for a damper-support member system, would be treated adequately by the present transfer function formulation. This problem is open to future research.

ACKNOWLEDGEMENTS

The present work was partially supported by Grant-in-Aid for Scientific Research (No. 07650659, No. 10555201 and No. 10650562) from the Ministry of Education, Science and Culture of Japan.

REFERENCES

1. I. Takewaki, 'Optimal damper placement for minimum transfer functions', *Earthquake Engng. Struct. Dynamics* **26**(11), 1113–1124 (1997).
2. T. Kobori *et al.*, 'Seismic-response-controlled structure with active mass driver system: Part 1 Design, Part 2 Verification', *Earthquake Engng. Struct. Dyn.* **20**, 133–149, 151–166 (1991).
3. T. Kobori, 'Structural control for large earthquakes', *Proc. IUTAM Symp.*, Kyoto, 1996, pp. 3–28.
4. K.K.F. Wong and G.C. Hart, 'Active control of inelastic structural response during earthquakes', *Struct. Des. Tall Buildings* **6**, 125–149 (1997).
5. T.T. Soong, 'Active structural control in civil engineering', *Engng. Struct.* **10**, 74–84 (1988).
6. G. Housner *et al.*, 'Special issue, Structural control: past, present, and future', *J. Engng. Mech. ASCE* **123**(9), 897–971 (1997).
7. M.C. Constantinou and I.G. Tadjbakhsh, 'Optimum design of a first story damping system', *Comput. Struct.* **17**(2), 305–310 (1983).
8. M. Gurgoze and P.C. Muller, 'Optimal positioning of dampers in multi-body systems', *J. Sound Vib.* **158**(3), 517–530 (1992).
9. R.H. Zhang and T.T. Soong, 'Seismic design of viscoelastic dampers for structural applications', *J. Struct. Engng. ASCE* **118**(5), 1375–1392 (1992).
10. G.D. Hahn and K.R. Sathiyaveeswaran, 'Effects of added-damper distribution on the seismic response of buildings', *Comput. Struct.* **43**(5), 941–950 (1992).
11. C.W. De Silva, 'An algorithm for the optimal design of passive vibration controllers for flexible systems', *J. Sound Vib.* **75**(4), 495–502 (1981).
12. J.A. Inaudi and J.M. Kelly, 'Optimum damping in linear isolation systems', *Earthquake Engng. Struct. Dyn.* **22**, 583–598 (1993).
13. M. Tsuji and T. Nakamura, 'Optimum viscous dampers for stiffness design of shear buildings', *Struct. Des. Tall Buildings* **5**, 217–234 (1996).
14. M. Tsuji and T. Nakamura, 'Stiffness design sequence of a shear building with Maxwell type viscous dampers for specified seismic drifts', *J. Struct. Construct. Engng AIJ* **491**, 55–64 (1997) (in Japanese).
15. S.F. Masri, G.A. Bekey and T.K. Caughey, 'Optimum pulse control of flexible structures', *J. Appl. Mech. ASME* **48**, 619–626 (1981).
16. A.K. Chopra, *Dynamics of Structures: Theory and Applications to Earthquake Engineering*, Prentice-Hall, Englewood Cliffs, NJ, 1995.
17. I. Takewaki, 'Efficient redesign of damped structural systems for target transfer functions', *Comput. Meth. Appl. Mech. Engng* **147**(3/4), 275–286 (1997).
18. I. Takewaki and K. Uetani, 'Optimal damper placement for building structures including surface ground amplification', *Proc. 13th ASCE EMD Conf.*, Baltimore, 1999.
19. N.M. Newmark and W.J. Hall, *Earthquake Spectra and Design*, Earthquake Eng. Research Institute, Berkeley, 1982.
20. J.N. Yang, S. Sarkani and F.X. Long, 'A response spectrum approach for seismic analysis of nonclassically damped structures', *Engng Struct.* **12**, 173–184 (1990).